Experimental Growth Law for Bubbles in a Moderately "Wet" 3D Liquid Foam

Jérôme Lambert, Isabelle Cantat, and Renaud Delannay
G.M.C.M. Université Rennes 1, CNRS UMR 6626, Bâtiment 11A, Campus Beaulieu 35042 Rennes Cedex, France

Rajmund Mokso and Peter Cloetens
Imaging Group-ESRF, BP 220, 38043 Grenoble Cedex 9, France

James A. Glazier
Department of Physics, Swain Hall West 159, Indiana University, 727 East Third Street, Bloomington, Indiana 47405-7105, USA

François Graner
Laboratoire de Spectrométrie Physique, CNRS UMR 5588, 140 Avenue de la physique, BP 87, 38402 Martin d'Hères, France
(Received 18 January 2007; published 2 August 2007)

We used x-ray tomography to characterize the geometry of all bubbles in a liquid foam of average liquid fraction $\phi_l \approx 17\%$ and to follow their evolution, measuring the normalized growth rate $\mathcal{G} = V^{-1/3}\frac{dV}{dt}$ for 7000 bubbles. While $\mathcal{G}$ does not depend only on the number of faces of a bubble, its average over f-faced bubbles scales as $G_f \sim f - f_0$ for large f's at all times. We discuss the dispersion of $\mathcal{G}$ and the influence of V and ϕ_l on $\mathcal{G}$.

DOI: 10.1103/PhysRevLett.99.058304 PACS numbers: 82.70.Rr, 83.80.Iz

Liquid foams consist of bubbles of gas separated by a continuous liquid phase occupying a fraction ϕ_l of the foam's volume. Liquid foams coarsen because gas slowly diffuses through the liquid films from high to low pressure bubbles, so the high pressure bubbles eventually disappear. The dynamics of the coarsening differs in the dry and infinitely wet limiting cases.

In a bubbly liquid with $\phi_l \sim 1$, bubbles are spherical and well separated. As in emulsions and diphasic materials, the bubbles coarsen via "Ostwald ripening" as theoretically described by Lifshitz, Slyozov, and Wagner (LSW) [1,2]. In the LSW regime, the change in volume of a bubble depends on its volume relative to an effective average volume.

In the dry-foam limit, $\phi_l \ll 1$, bubbles are polyhedral and touch each other. The gas flux between two neighboring bubbles is proportional to their pressure difference, hence to the mean curvature of the film separating them. From simple dimensional arguments [3], the growth rate of an individual bubble of volume V in a 3D foam must be of the form

$$\frac{dV}{dt} = V^{1/3}\mathcal{G}. \tag{1}$$

$\mathcal{G}$ depends both on the shape of the bubble and on the physico-chemical characteristics of the liquid, gas, and surfactant, which we aggregate into an *effective gas diffusivity* D_{eff}, so that we can rewrite Eq. (1) as

$$\mathcal{G} = -D_{\text{eff}} \int_S \frac{H dS}{V^{1/3}}, \tag{2}$$

where H is the mean curvature of a surface element dS of the bubble. Theoretical treatments of coarsening in dry foams usually make an analogy with 2D foams, for which von Neumann's law (vNM), which is exact, states that the growth rate of the area of a bubble is proportional to $n - 6$, where n is its number of edges. This law has been validated experimentally [4]. In 3D, in contrast, the existence of the extra radius of curvature means that the growth rate of a bubble needs not depend only on its number of faces [5,6]. MacPherson and Srolovitz recently related dV/dt for a bubble in a dry foam to a characteristic length for the bubble and the sum of the lengths of its edges [7]. This result should aid future experimental analysis since measuring edge length is substantially easier than measuring surface curvature in pixel-based images.

Attempts to relate the growth rates of individual bubbles or the average growth rates of classes of bubbles to simple geometrical properties of individual bubbles have had mixed success. Mullins [8] and several groups (see [5] and references therein) derived analytical (assuming idealized regular bubbles) or numerical (using the finite element software package SURFACE EVOLVER [9]) estimates for $\mathcal{G}$ from the rhs of Eq. (2) and obtained $\mathcal{G}_M \sim f^{1/2}$ for large f. On the other hand, numerical simulations of coarsening have computed $\mathcal{G}$ from the left-hand side of Eq. (1) for large numbers of bubbles. Potts model [3,10], vertex model [11], and SURFACE EVOLVER [12] simulations all exhibit a strong correlation between the bubbles' number of faces and growth rates, with a small dispersion due to the intrinsic foam dynamics rather than to numerical or counting error. We would expect to be able to check if the Mullins model holds on average for coarsening foams by evaluating the average values $G_f = \langle \mathcal{G} \rangle_f$ over sets of f-faced bubbles. Unfortunately, existing numerical

 © 2007 The American Physical Society

data admit both $G_f \sim (f - f_0)$ and $G_f \sim (f - f_0)^{1/2}$ fits. Similarly, experimental measurements of G_f using optical tomography [13,14] and NMR [15–18] observed too few bubbles to distinguish $(f - f_0)$ from $(f - f_0)^{1/2}$.

In this Letter, we investigate foam coarsening experimentally in the intermediate wetness regime with $\phi_l \sim$ 10%–20%. This regime has not been studied theoretically or computationally, but is that used in most real-world foam applications [19,20]. We determine $\mathcal{G}$ and G_f for several thousand bubbles at wetnesses at which we might expect to see behavior intermediate between the LSW and vNM regimes. Recent progress in x-ray tomography [21] permits us to take 3D images of thousands of bubbles in 2 min, and allows us to monitor a foam for many hours. We find that, for a given set of f-faced bubbles, the dispersion of $\mathcal{G}$ is small. Therefore we focus on G_f. While the shape of the distribution of the number of faces per bubble changes during the experiment (implying that our foam has not reached a statistically-invariant scaling state), the shape of G_f vs f stays constant. This function thus seems to be a robust way to characterize wet foam coarsening. G_f depends linearly on f for large f. We also show that $\mathcal{G}$ depends on V, as we expect, since V and f correlate, but this dependence weakens as the liquid fraction decreases.

The x-ray tomography apparatus at the ID19 beam line of the European Synchrotron Radiation facility (ESRF) Grenoble, France, enables us to visualize the coarsening of a wet liquid foam contained in a 1 cm high by 1 cm diameter cylindrical volume. The spatial resolution of the images is 10 μm in each direction, smaller than the smallest bubbles which appear in at least two successive images (i.e., any bubble smaller than 10 μm in diameter disappears in less than 2 minutes and thus never enters our calculations of growth rates). Thus we can image all bubbles which we can analyze (by definition, we do not include in G_f bubbles which disappear within one time step). Since the liquid phase occupies only a small fraction ϕ_l of the total volume, obtaining adequate image contrast is difficult: we use an x-ray beam energy of 15 keV, which optimizes contrast. In addition, the bubble walls must not move significantly during the time required to acquire an image or tomographic reconstruction of the foam will fail. The characteristic evolution time for gas diffusion in $\sim$1 mm^3 air bubbles is several minutes, permitting reconstruction of all but the smallest bubbles. Our experimental acquisition time of 2 min per image enabled us to clearly identify and follow bubbles during their evolution. To reduce the complicating effects of gravitational drainage of the foam and to maintain a constant and relatively high liquid fraction, we used a high-viscosity liquid composed of 100 ml deionized water, 0.1 g sodium dodecyl phosphate, 0.003 g dodecanol and 1 g gelatin (not enough to gel the liquid). In addition, we used a pump to provide a constant supply of liquid to the top of the foam, which, within 48 min, produced a fairly stable liquid-fraction gradient, decreasing from 20% at the top to 10% at the bottom [21].

We identified bubbles in a reconstructed tomographic image using a watershed method detailed in [21]. We measured the liquid fraction in a region by summing the number of pixels in that volume containing more than a threshold amount of liquid, allowing us to estimate ϕ_l with an error $\Delta\phi_l = 0.5\%$. This method produces a very few ($\ll 5\%$) spurious small bubbles due to noise in the reconstructed tomographic images. We checked that they did not affect our results by introducing a size cutoff to eliminate small bubbles and recalculating our derived quantities. All of our results stayed within error of the unfiltered data (data not shown). We developed a correlation algorithm using the commercial APHELION [22] software package to track bubbles from image to image, enabling us to determine their growth rates.

In a wet foam, in the presence of large *vertices* (the meeting points of edges of neighboring bubbles), a bubble's number of faces can be ambiguous [21]. To resolve this ambiguity, we compared the distance separating two bubbles to the characteristic size of their vertices and assumed that if the distance was less than half the size, they were neighbors and shared a face. This definition permits small bubbles located at vertices to have fewer than four faces. We automatically discarded from our analysis bubbles which touched the container walls.

To test the influence of the liquid fraction on foam dynamics, we defined four subregions corresponding to different heights and thus wetnesses in our column.

For each image, we measured each bubble's number of faces f and growth rate $\mathcal{G}$. Figure 1 shows $\mathcal{G}$ vs f for the 3582 bubbles in the topmost horizontal slice of the cell 48 min after foam creation. Because we are measuring small differences between fairly large successive Vs, the errors in $\mathcal{G}$ can be large even for relatively small errors in V. We estimated our error for $\mathcal{G}$ by assuming a worst-case error in our measurement of V, defining ΔV to be the error resulting from dilating or eroding complete faces of each bubble by one voxel (our actual errors in determining the positions of faces tend to cancel, so this estimate is conservative).

$\mathcal{G}$ varies for different bubbles with the same fs to a much greater extent than the experimental uncertainty. Hence $\mathcal{G}$ is not an exact function of f, even though the two quantities correlate, showing that 3D wet bubbles do not obey an exact equivalent of von Neumann's law involving only a bubble's number of faces. However, for the ensemble of bubbles with a given f, the dispersion of $\mathcal{G}$ around its average is not large, as the inset in Fig. 1 shows for $f = 12$, since we clearly see an increase of $\mathcal{G}$ with f: the dispersion $\sigma_{\mathcal{G}}$ coincides with the variation of G_f for $\Delta f \approx 5$ (with $f > 10$). We therefore investigate G_f's dependence on ϕ_l and the structure of the foam.

Foam structure changes during coarsening. We characterize the structure by measuring the distribution of bub-

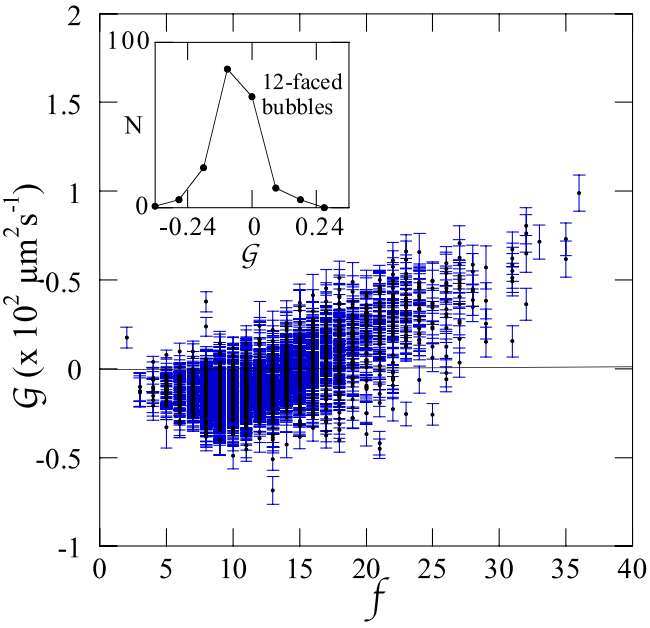

FIG. 1 (color online). Scatter plot of $\mathcal{G}$ vs f in the topmost slice ($\phi_l = 20\%$) of the experimental cell. Inset: histogram of $\mathcal{G}$ for 12-faced bubbles.

bles' number of faces $\rho(f)$. Figure 2 shows $\rho(f)$ at different times and for different values of ϕ_l.

The shape of the distribution varies significantly with time and liquid fraction. The average number of neighbors, $\langle f \rangle$ ranges from 10.7 ± 5.5 ($\phi_l = 20\%$) to 11.0 ± 4.5 ($\phi_l = 14\%$). Figure 2 also shows that $\rho(f)$ varies signifi-

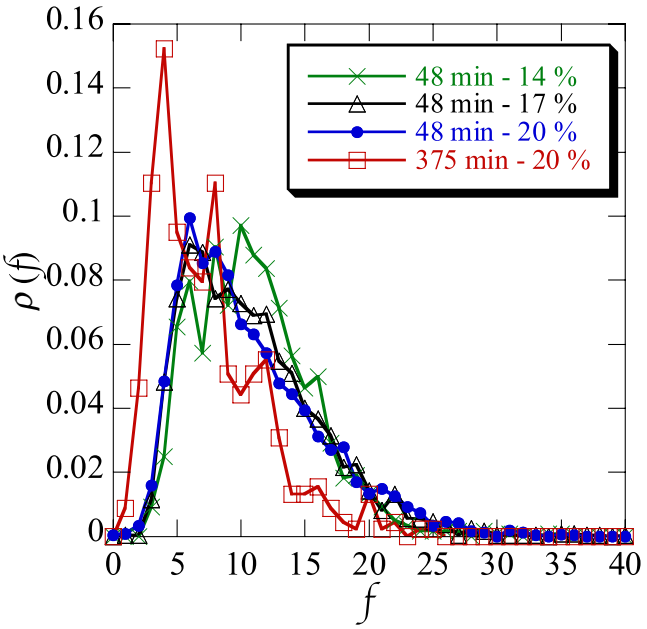

FIG. 2 (color online). Red and blue lines: $\rho(f)$ for $\phi_l = 20\%$, 48 min (3582 bubbles) and 375 min (454 bubbles) after foam creation. Green and black lines: $\rho(f)$ for $\phi_l = 14\%$ (1207 bubbles) and 17% (2451 bubbles), 48 min after foam creation.

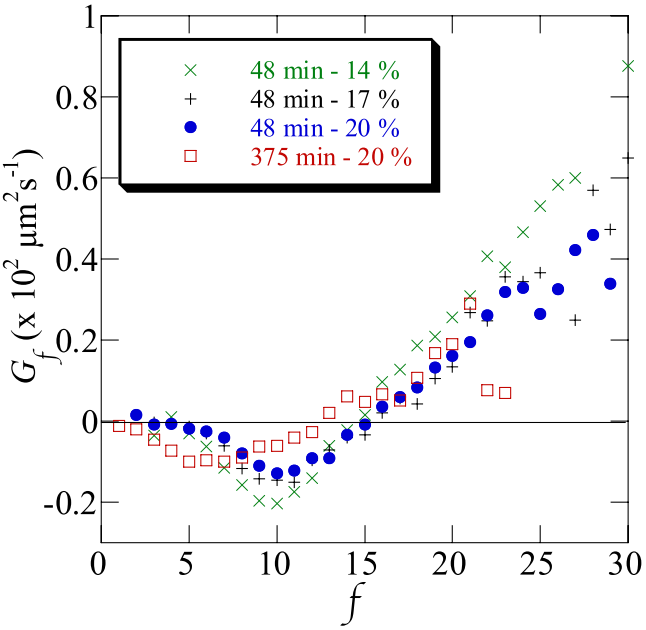

FIG. 3 (color online). Blue and red points: G_f vs f, 48 min and 375 min after foam creation, for $\phi_l = 20\%$. Green and black points: G_f vs f, 48 min after foam creation, for $\phi_l = 14\%$ and $\phi_l = 17\%$.

cantly from 48 min to 375 min after foam creation; hence, the structure is still far from a scale-invariant regime [10,12] [in which the characteristic size $\langle V \rangle(t)$ grows in time and $\rho(f)$ is constant, as well as all distributions and correlations, made nondimensional by rescaling by appro-

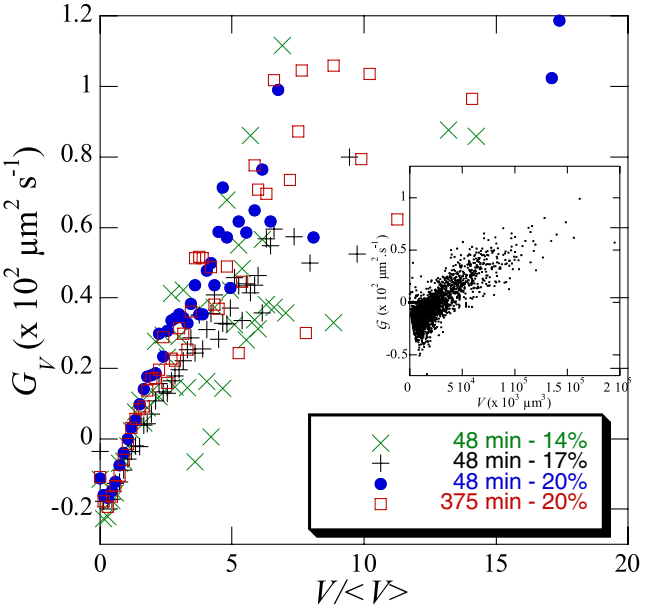

FIG. 4 (color online). Blue and red points: G_V vs $V/\langle V \rangle$, 48 min and 375 min after foam creation, for $\phi_l = 20\%$. Green and black points: G_V vs V, 48 min after foam creation, for $\phi_l = 14\%$ and $\phi_l = 17\%$. Inset: $\mathcal{G}$ vs V for $\phi_l = 20\%$, 48 after foam creation.

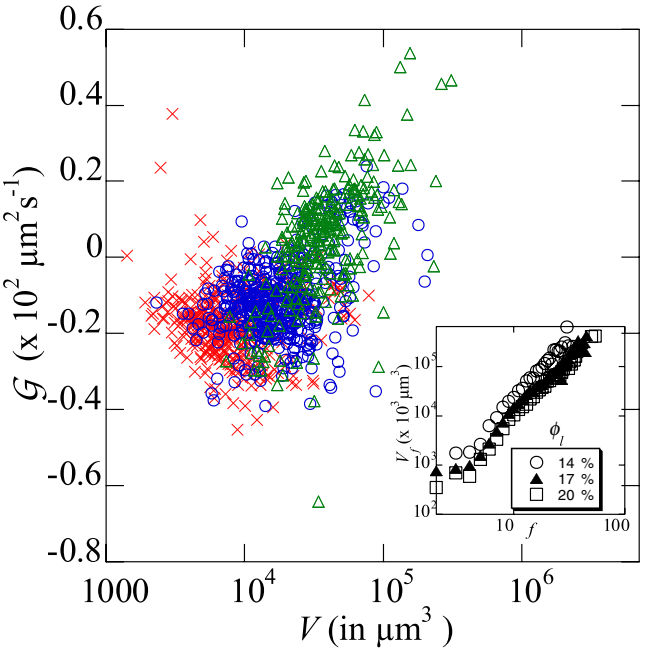

FIG. 5 (color online). Scatter plot of the growth rate $\mathcal{G}$ vs V for 8- (red), 12- (blue) and 16-faced (green) bubbles. Inset: $\langle V \rangle_f$ as a function of f for $\phi_l = 14$, 17 and 20%.

priate powers of $\langle V \rangle(t)$]. The foams contains too few bubbles at later stages to compute statistically-relevant G_fs. Figure 3 shows G_f at two different times for different values of ϕ_l. Despite a shift in the value of f at which G_f crosses 0, spotting the f below which, on average, bubbles shrink into large f bubbles, the general dependence of G_f on f is unchanged: G_f goes to 0 as $f \to 0$ for $f < 10$, and G_f is linear for $f > 10$. We also checked that G_f is linear in f during the early stages of foam evolution (data not shown). Since in the limit $\phi_l \to 1$, $\mathcal{G}$ should depend on V only, we plot G_V vs $V/\langle V \rangle$ in Fig. 4, where G_V is the average of $\mathcal{G}$ over bubbles contained in the same 0.15-wide $V/\langle V \rangle$ bin. As we expect, the quantities correlate. The dispersion of G_V increases as ϕ_l decreases. While the $\mathcal{G}$ values for $\phi_l = 20\%$ cluster tightly (see the inset in Fig. 4), the $\mathcal{G}$ values for $\phi_l = 14\%$ are much more dispersed. Finally, we scatter plot $\mathcal{G}$ vs V for three different sets of f-faced bubbles in Fig. 5. For fixed f, $\mathcal{G}$ increases slightly with V. The shift along the V axis of the clouds of $\mathcal{G}$s corresponding to particular values of f results from the strong correlation between $\langle V \rangle_f$ and f shown in the inset of Fig. 5 [10,12,19].

We find a power law relation between $\langle V \rangle_f$ and f: $V_f = \langle V \rangle_f \sim f^\alpha$, with $\alpha \approx 2.2$, close to the 2.25 observed in SURFACE EVOLVER [23] or Potts model [10] simulations of dry foams.

Our experiments studied a moderately wet foam ($14\% < \phi_l < 20\%$), a class of foam for which we have no theoretically or computationally predicted dynamics. $\mathcal{G}$ is not a well-defined function of f and G_f disagrees with prior mean-field theories for both wet and dry foams. As in dry-foam Potts model simulations of coarsening [3,10], G_f increases to zero as f decreases for small fs and increases linearly with f for large fs.

[1] I. Lifshitz and V. Slyozov, J. Phys. Chem. Solids **19**, 35 (1961).
[2] C. Wagner, Z. Elektr. Inf.-Energietech. **65**, 581 (1961).
[3] J. Glazier, Phys. Rev. Lett. **70**, 2170 (1993).
[4] J. A. Glazier, S. P. Gross, and J. Stavans, Phys. Rev. A **36**, 306 (1987).
[5] S. Jurine, S. Cox, and F. Graner, Colloids Surf. A **263**, 18 (2005).
[6] J. A. Glazier and B. Prause, in *Foams, Emulsion and Their Application (Proceedings of the Eurofoam Conference, Delft 2002)*, edited by P. Zitha (Verlag MIT, Bremen, 2000), p. 120.
[7] R. D. MacPherson and D. J. Srolovitz, Nature (London) **446**, 1053 (2007).
[8] W. W. Mullins, Acta Metall. **37**, 2979 (1989).
[9] See K. Brakke, http://www.susqu.edu/facstaff/b/brakke/evolver/.
[10] G. L. Thomas, R. M. C. de Almeida, and F. Graner, Phys. Rev. E **74**, 021407 (2006).
[11] K. Fuchizaki and K. Kawazaki, Physica (Amsterdam) **221A**, 202 (1995).
[12] F. Wakai, N. Enomoto, and H. Ogawa, Acta Mater. **48**, 1297 (2000).
[13] C. Monnereau and M. Vignes-Adler, Phys. Rev. Lett. **80**, 5228 (1998).
[14] C. Monnereau and M. Vignes-Adler, J. Colloid Interface Sci. **202**, 45 (1998).
[15] C. P. Gonatas, J. S. Leigh, A. G. Yodh, J. A. Glazier, and B. Prause, Phys. Rev. Lett. **75**, 573 (1995).
[16] B. Prause, J. A. Glazier, S. Gravina, and C. Montemagno, Condens. Matter Phys. **7**, L511 (1995).
[17] B. Prause and J. A. Glazier, in *Proceedings of the 5th Experimental Chaos Conference, Orlando*, edited by M. Ding, W. L. Ditto, L. M. Pecora, and M. L. Spano (World Scientific, Singapore, 2001), p. 427.
[18] B. A. Prause, Ph.D. thesis, University of Notre Dame, 2000.
[19] D. Weaire and S. Hutzler, *The Physics of Foams* (Oxford University, Oxford, 2000).
[20] *Foams, Theory, Measurements and Applications*, edited by R. K. Prud'homme and S. A. Khan (Marcel Dekker, New York, 1996).
[21] J. Lambert, I. Cantat, R. Delannay, A. Renault, F. Graner, J. A. Glazier, I. Veretennikov, and P. Cloetens, Colloids Surf. A **263**, 295 (2005).
[22] http://www.adcis.net.
[23] A. M. Kraynik, D. A. Reinelt, and F. van Swol, Phys. Rev. Lett. **93**, 208301 (2004).